Fan, Boran and Wang, Kui and Gu, Chunyang and Wheeler, Patrick and Li, Yongdong (2016) A branch current reallocation based energy balancing strategy for the modular multilevel matrix converter operating around equal frequency. In: 42nd Annual Conference of IEEE Industrial Electronics Society (IECON 2016), 24-27 Oct 2016, Florence, Italy.

A Branch Current Reallocation Based Energy Balancing Strategy for the Modular Multilevel Matrix Converter Operating Around Equal Frequency

Boran Fan [1], Kui Wang [1], Chunyang Gu [2], Pat Wheeler [2], Yongdong Li [1]
[1]State Key Lab of Power System, Dept. of Electrical Engineering, Tsinghua University, Beijing, China
[2]Department of Electrical and Electronic Engineering, University of Nottingham, Nottingham, United Kingdom
E-mail: fbr13@mails.tsinghua.edu.cn

***Abstract*—The Modular multilevel matrix converter (M3C) is a promising topology for medium-voltage, high-power applications. Due to the modular structure, it is scalable, produces high quality output waveforms and can be fault tolerant. However, the M3C suffers from capacitor-voltage fluctuation if the output frequency is similar to the input frequency. This problem could limit the circuit's application in the adjustable speed drives (ASD). This paper introduces a theoretical analysis in the phasor-domain to find the branch energy equilibrium point of the M3C when operating with equal input and output frequencies. On the basis of this equilibrium point, a branch current reallocation based energy balancing control method is proposed to equalize the energy stored in the nine converter branches. With this novel control method, the M3C can effectively overcome the capacitor voltage fluctuation without using balancing techniques based on common mode voltage or applying reactive power at the input side.**

Keywords—modular multilevel matrix converter (M3C); energy and balancing control; equal frequency

I. INTRODUCTION

The modular multilevel matrix converter (M3C), shown in Fig. 1, can be used to connect two three-phase electrical systems (input-side and output-side) using nine active branches. Each branch is formed of a cascaded connection of full-bridge (H-bridge) converter cells. The topology enables direct AC-AC bidirectional power conversion and ensures that the average three-phase input and output waveforms are sinusoidal with controllable displacement factor on the input side [1]-[4]. In common with other members of the modular multilevel cascade converter (MMCC) family, the voltage ratings of the M3C can be increased by adding additional cascaded cells. The M3C is more suitable for low-speed constant-torque motor drives than the modular multilevel converters (MMC) in back-to-back configuration [5], [6]. These advantages make the M3C a promising topology for the medium-voltage, high-power adjustable speed drive (ASD) applications. However, the M3C suffers from capacitor voltage fluctuation if the output frequency is similar to the input frequency. This voltage fluctuation can be at a very low frequency (the difference between input and output frequencies). The result is a power difference between the branches and as a result, an unbalance in the energy stored in each branch.

In order to solve this problem, [2] presents a solution by both injecting circulating current into M3C and applying reactive power at the input side. However, the reactive power at the input side is not allowed in some applications as the input side is normally connected to the electrical grid. The work described in [4] introduces some common voltage to avoid the need for reactive power at the input side, a similar technique to the mitigation control of the MMC at low-speed range [7]. However, the reference for the common voltage is difficult to design and may cause over-modulation. The common mode voltage may also lead to premature failure of motor bearings. The ideas described in [8] use an adjustment in the motor voltage to ensure that the input and output side share the same voltage magnitude. This method helps to achieve lower branch currents but has some operational restrictions and also needs reactive power at the input side.

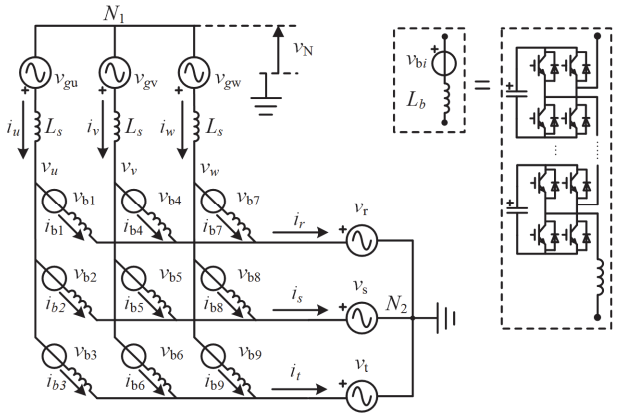

Fig. 1. Circuit Configuration of the M3C

As reactive power at the input side is not allowed in some applications and the common mode voltage may cause serious problems, this paper presents an alternative control method that only uses the circulating currents in the M3C to equalize the energy within the nine branches. This paper proves the viability of this solution and then develops a strategy to design specifically appropriate circulating currents. With this control method, the M3C can effectively overcome the capacitor

voltage fluctuation issue without using common mode voltage or applying reactive power at the input side. The proposed control strategy has been validated using simulation results.

II. BASIC THEORY OF THE M3C

A. Double αβ0 Transformation

In the M3C there are four independent inner circulating currents [1]-[4]. These circulating currents are independent of input side currents (i_u, i_v, i_w) and output side currents (i_r, i_s, i_t). Power transfer between different branches is realized by adjusting the value of these 4 circulating currents. Theoretically, there are multiple definitions of these circulating currents. In recent literatures, by introducing a so-called double αβ0 transformation to M3C, circulating currents are defined as $i_{\alpha\alpha}$, $i_{\alpha\beta}$, $i_{\beta\alpha}$ and $i_{\beta\beta}$. The definition of the double αβ0 transformation $T_{Dual\text{-}\alpha\beta}$ is in (1).

$$\mathbf{T_{Dual\text{-}\alpha\beta}(M_{3*3})} = \mathbf{T_{ab}} \cdot \mathbf{M_{3*3}} \cdot \mathbf{T_{ab}}^{\mathbf{T}},\ \mathbf{T_{ab}} = \begin{bmatrix} \frac{2}{3} & -\frac{1}{3} & -\frac{1}{3} \\ 0 & \frac{\sqrt{3}}{3} & -\frac{\sqrt{3}}{3} \\ \frac{1}{3} & \frac{1}{3} & \frac{1}{3} \end{bmatrix} \quad (1)$$

Usng the double αβ0 transformation on the nine branch currents and gets the $i_{\alpha\alpha}$, $i_{\alpha\beta}$, $i_{\beta\alpha}$ and $i_{\beta\beta}$ in (2). Here $i_{\alpha0}$ and $i_{\beta0}$ are components of the input currents on the α-axis and β-axis and $i_{\alpha0}$ and $i_{\beta0}$ are components of the output currents on the α-axis and β-axis.

$$\begin{bmatrix} i_{\alpha\alpha} & i_{\alpha\beta} & i_{\alpha0} \\ i_{\beta\alpha} & i_{\beta\beta} & i_{\beta0} \\ i_{0\alpha} & i_{0\beta} & i_{00} \end{bmatrix} = \mathbf{T_{ab}} \begin{bmatrix} i_{b1} & i_{b2} & i_{b3} \\ i_{b4} & i_{b5} & i_{b6} \\ i_{b7} & i_{b8} & i_{b9} \end{bmatrix} \mathbf{T_{ab}}^{\mathbf{T}} \quad (2)$$

The double αβ0 transformation also helps to realize a decoupled control of these four circulating currents as shown in Fig. 2 [9]. Using simple proportional-integral (PI) regulators, the $i_{\alpha\alpha}$, $i_{\alpha\beta}$, $i_{\beta\alpha}$ and $i_{\beta\beta}$ are easily controlled by $v_{\alpha\alpha}$, $v_{\alpha\beta}$, $v_{\beta\alpha}$ and $v_{\beta\beta}$. Here, voltage $v_{\alpha\alpha}$, $v_{\alpha\beta}$, $v_{\beta\alpha}$ and $v_{\beta\beta}$ are defined in (3).

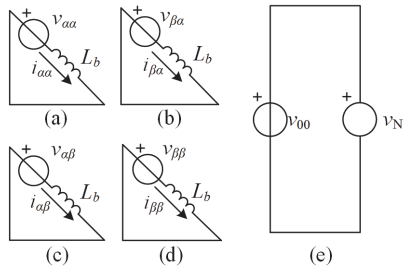

Fig. 2. Circulating currents and common-voltage in the M3C

$$\begin{bmatrix} v_{\alpha\alpha} & v_{\alpha\beta} & v_{\alpha0} \\ v_{\beta\alpha} & v_{\beta\beta} & v_{\beta0} \\ v_{0\alpha} & v_{0\beta} & v_{00} \end{bmatrix} = \mathbf{T_{ab}} \begin{bmatrix} v_{b1} & v_{b2} & v_{b3} \\ v_{b4} & v_{b5} & v_{b6} \\ v_{b7} & v_{b8} & v_{b9} \end{bmatrix} \mathbf{T_{ab}}^{\mathbf{T}} \quad (3)$$

The value of the common voltage v_N in Fig. 1 is equal to the value of v_{00} as shown in Fig. 2. In order to avoid common-voltage, according to (1) and (3), the value of v_{00} satisfies (4).

$$v_N = v_{00} = \frac{1}{9}\sum_{i=1}^{9} v_{bi} \triangleq 0 \quad (4)$$

B. Basic Branch Current Allocation

If control circulating currents $i_{\alpha\alpha}$, $i_{\alpha\beta}$, $i_{\beta\alpha}$ and $i_{\beta\beta}$ all to be zero, the nine branch currents would be (5). The branch current consists of 1/3 of the *x*-phase (*x*=u,v,w) input side current and 1/3 of the *y*-phase (*y*=r,s,t) output side current.

$$\begin{bmatrix} i_{b0,1} & i_{b0,2} & i_{b0,3} \\ i_{b0,4} & i_{b0,5} & i_{b0,6} \\ i_{b0,7} & i_{b0,8} & i_{b0,9} \end{bmatrix} = \frac{1}{3} \cdot \begin{bmatrix} i_u & i_u & i_u \\ i_v & i_v & i_v \\ i_w & i_w & i_w \end{bmatrix} + \frac{1}{3} \cdot \begin{bmatrix} i_r & i_s & i_t \\ i_r & i_s & i_t \\ i_r & i_s & i_t \end{bmatrix} \quad (5)$$

In this paper, the branch currents in (5) are defined as the "basic branch current". Recent literatures mostly assume this branch current allocation as the branch energy equilibrium point. On the basis of this allocation, circulating currents $i_{\alpha\alpha}$, $i_{\alpha\beta}$, $i_{\beta\alpha}$ and $i_{\beta\beta}$ are designed to compensate possible branch energy difference.

C. Capacitor-voltage Fluctuation

The input and output systems are assumed to be three-phase balanced and with positive sequence. No reactive power is applied at the input side. Voltages and currents at the input and output side are defined as,

$$v_u = \hat{v}_{m1}\cos(\omega_1 t) \quad (6)$$

$$i_u = \hat{i}_{m1}\cos(\omega_1 t) \quad (7)$$

$$v_r = \hat{v}_{m2}\cos(\omega_2 t + \theta) \quad (8)$$

$$i_r = \hat{i}_{m2}\cos(\omega_2 t + \theta - \varphi) \quad (9)$$

Applying the basic branch currents allocation defined in (5), the power on branch 1, for instance, is shown in (10). This branch power consists of frequency components of ω_1-ω_2, ω_1+ω_2, $2\omega_1$, $2\omega_2$.

$$\begin{aligned} p_{b1} &= (v_u - v_r)\cdot(i_u + i_r)/3 \\ &= p|_{\omega=\omega1-\omega2} + \underbrace{p|_{\omega=\omega1+\omega2} + p|_{\omega=2\omega1} + p|_{\omega=2\omega2}}_{p_h} \end{aligned} \quad (10)$$

When output side frequency (ω_2) gets close to the input side frequency (ω_1), the low-frequency power component of ω_1-ω_2 causes large branch energy fluctuation. This power component is shown in (11) and (12). In conclusion, when operating M3C around equal frequency, applying the basic branch currents allocation causes large branch energy fluctuation. Therefore a branch currents reallocation should be developed.

$$p\,|_{\omega=\omega 1-\omega 2} = \frac{\sqrt{\hat{v}_{m1}^2\hat{i}_{m2}^2+\hat{v}_{m2}^2\hat{i}_{m1}^2-2\hat{v}_{m1}\hat{v}_{m2}\hat{i}_{m1}\hat{i}_{m2}\cos\varphi}}{6}\cdot\cos[(\omega_1-\omega_2)t-\theta+\delta] \quad (11)$$

$$\delta=\arctan\left(\frac{\hat{v}_{m1}\hat{i}_{m2}\sin\varphi}{\hat{v}_{m1}\hat{i}_{m2}\cos\varphi-\hat{v}_{m2}\hat{i}_{m1}}\right) \quad (12)$$

III. BRANCH ENERGY EQUILIBRIUM POINT OF M3C WHEN OPERATING AROUND EQUAL FREQUENCY

A. *Phasor-domain Analysis of the M3C*

In this section an analysis is presented in the phasor-domain instead of time-domain. This helps to visualize the analysis of branch energy balancing for the equal-frequency operation. Assuming $\omega_1=\omega_2$, rewritten the definition of (6)-(9) in phasor-domain,

$$\vec{v}_u=\hat{v}_{m1}\cdot e^{j\cdot 0} \quad (13)$$

$$\vec{i}_u=\hat{i}_{m1}\cdot e^{j\cdot 0} \quad (14)$$

$$\vec{v}_r=\hat{v}_{m2}\cdot e^{j\cdot\theta} \quad (15)$$

$$\vec{i}_r=\hat{i}_{m2}\cdot e^{j\cdot(\theta-\varphi)} \quad (16)$$

The basic branch currents in phasor-domain would be,

$$\begin{bmatrix}\vec{i}_{b0,1} & \vec{i}_{b0,2} & \vec{i}_{b0,3}\\ \vec{i}_{b0,5} & \vec{i}_{b0,6} & \vec{i}_{b0,4}\\ \vec{i}_{b0,9} & \vec{i}_{b0,7} & \vec{i}_{b0,8}\end{bmatrix}=\frac{1}{3}\begin{bmatrix}\vec{i}_u & \vec{i}_u & \vec{i}_u\\ \vec{i}_v & \vec{i}_v & \vec{i}_v\\ \vec{i}_w & \vec{i}_w & \vec{i}_w\end{bmatrix}+\frac{1}{3}\begin{bmatrix}\vec{i}_r & \vec{i}_s & \vec{i}_t\\ \vec{i}_r & \vec{i}_s & \vec{i}_t\\ \vec{i}_r & \vec{i}_s & \vec{i}_t\end{bmatrix} \quad (17)$$

In (18), $\vec{e}_{ni}\ (i=1,2,..9)$ is the unit length phasor that leads branch voltage $\vec{v}_{bi}(i=1,2,..9)$ by 90º as in (19).

$$[\mathbf{e_n}]=\begin{bmatrix}\vec{e}_{n1} & \vec{e}_{n2} & \vec{e}_{n3} & \vec{e}_{n4} & \vec{e}_{n5} & \vec{e}_{n6} & \vec{e}_{n7} & \vec{e}_{n8} & \vec{e}_{n9}\end{bmatrix}^T \quad (18)$$

$$\vec{e}_{ni}=\frac{\vec{v}_{bi}}{|\vec{v}_{bi}|}\cdot j\triangleq e^{j\cdot\sigma_{bi}}=\cos\sigma_{bi}+j\cdot\sin\sigma_{bi},\ (i=1,2,..9) \quad (19)$$

Here $[\mathbf{e_n}]$ is separated into three groups as $[\mathbf{e_{n1,5,9}}]$, $[\mathbf{e_{n2,6,7}}]$ and $[\mathbf{e_{n3,4,8}}]$. In each group, $\vec{e}_{n1}/\vec{e}_{n2}/\vec{e}_{n3}$ leads $\vec{e}_{n5}/\vec{e}_{n6}/\vec{e}_{n4}$ 120º and $\vec{e}_{n5}/\vec{e}_{n6}/\vec{e}_{n4}$ leads $\vec{e}_{n9}/\vec{e}_{n7}/\vec{e}_{n8}$ 120º respectively as in (20)-(22).

$$[\mathbf{e_{n1,5,9}}]=\begin{bmatrix}\vec{e}_{n1} & \vec{e}_{n5} & \vec{e}_{n9}\end{bmatrix}=\vec{e}_{n1}\cdot\begin{bmatrix}1 & e^{j\alpha} & e^{j2\alpha}\end{bmatrix} \quad (20)$$

$$[\mathbf{e_{n2,6,7}}]=\begin{bmatrix}\vec{e}_{n2} & \vec{e}_{n6} & \vec{e}_{n7}\end{bmatrix}=\vec{e}_{n2}\cdot\begin{bmatrix}1 & e^{j\alpha} & e^{j2\alpha}\end{bmatrix} \quad (21)$$

$$[\mathbf{e_{n3,4,8}}]=\begin{bmatrix}\vec{e}_{n3} & \vec{e}_{n4} & \vec{e}_{n8}\end{bmatrix}=\vec{e}_{n3}\cdot\begin{bmatrix}1 & e^{j\alpha} & e^{j2\alpha}\end{bmatrix} \quad (22)$$

Fig. 3 is the phasor diagram of the M3C, input side voltage and currents in (13) and (14) are shown in red color; output side voltage and currents in (15) and (16) are shown in green color; basic branch currents in (17) are shown in purple color; $[\mathbf{e_n}]$ are shown in blue color. Obviously, in order to stabilize branch energies, there should be no active power on each branch. Therefore the branch current phasor $\vec{i}_{bi}(i=1,2,..9)$ should be in the same or opposite direction with $\vec{e}_{ni}(i=1,2,..9)$. This condition is explain in (23)-(25). Here $[\mathbf{C}]$ is the vector of nine branch currents magnitude.

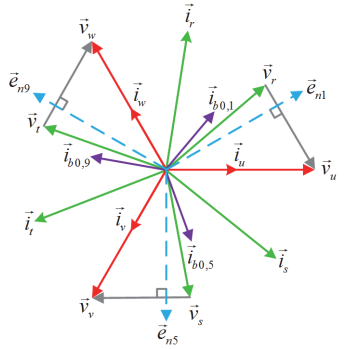

(a)

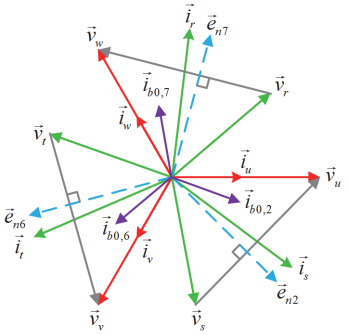

(b)

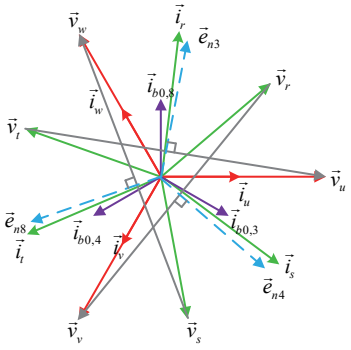

(c)

Fig. 3. Phasor Diagram of the M3C

(a) Branch 1,5,9 (b) Branch 2,6,7 (c) Branch 3,4,8

However, in Fig. 3 the basic branch current phasors are clearly with phase difference to $[\mathbf{e_n}]$ and do not meet the condition in (23). This causes a branch energy derivation when $\omega_1=\omega_2$ and a large branch energy fluctuation when $\omega_1\approx\omega_2$. This result is consist with the analysis in time-domain as explain in PART II.C.

$$[\mathbf{i_b}]=[\mathbf{C}]\cdot[\mathbf{e_n}] \quad (23)$$

$$[\mathbf{i_b}]=\begin{bmatrix}\vec{i}_{b1} & \vec{i}_{b2} & \vec{i}_{b3} & \vec{i}_{b4} & \vec{i}_{b5} & \vec{i}_{b6} & \vec{i}_{b7} & \vec{i}_{b8} & \vec{i}_{b9}\end{bmatrix}^T \quad (24)$$

$$[\mathbf{C}]=\begin{bmatrix}c_1 & c_2 & c_3 & c_4 & c_5 & c_6 & c_7 & c_8 & c_9\end{bmatrix} \quad (25)$$

B. Branch Current Magnitude Calculation

As input and output side are three-phase balanced, the value of branch current magnitudes c_1, c_5 and c_9 are equal and so as c_2, c_6, c_7 and c_3, c_4, c_8 as shown in (26).

$$c_1=c_5=c_9,\ c_2=c_6=c_7,\ c_3=c_4=c_8 \quad (26)$$

Branch currents satisfy,

$$\vec{i}_u=\vec{i}_{b1}+\vec{i}_{b2}+\vec{i}_{b3}=c_1\cdot\vec{e}_{n1}+c_2\cdot\vec{e}_{n2}+c_3\cdot\vec{e}_{n3} \quad (27)$$

$$\vec{i}_r=\vec{i}_{b1}+\vec{i}_{b4}+\vec{i}_{b7}=c_1\cdot\vec{e}_{n1}+c_2\cdot e^{j2\alpha}\cdot\vec{e}_{n2}+c_3\cdot e^{j\alpha}\cdot\vec{e}_{n3} \quad (28)$$

Combined with (14) and (16), the branch currents magnitudes satisfy,

$$\mathbf{[A][C]=[B]} \quad (29)$$

Where,

$$\mathbf{[A]}=\begin{bmatrix}\sin\sigma_{b1} & \sin\sigma_{b2} & \sin\sigma_{b3}\\ \sin\sigma_{b1} & \sin(\sigma_{b2}+2\alpha_n) & \sin(\sigma_{b3}+\alpha_n)\\ \cos\sigma_{b1} & \cos(\sigma_{b2}+2\alpha_n) & \cos(\sigma_{b3}+\alpha_n)\end{bmatrix},\quad \alpha_n=-\frac{2}{3}\pi \quad (30)$$

$$\mathbf{[B]}=\begin{bmatrix}0 & \hat{i}_{m2}\cdot\sin(\theta-\varphi) & \hat{i}_{m2}\cdot\cos(\theta-\varphi)\end{bmatrix} \quad (31)$$

Branch current magnitudes are obtained by solving this equation. Assuming $\mathbf{[C]}^*$ is a possible solution of (29), combined with (23) the reallocated branch currents should be $[\mathbf{i_b}]^*=[\mathbf{C}]^*\cdot[\mathbf{e_n}]$. In this paper, $[\mathbf{i_b}]=[\mathbf{i_b}]^*$ is called as the branch energy equilibrium point of M3C when operating around equal frequency

C. Disscussion on the Control Availability

This section describes the development of a control method only using circulating currents in the M3C to equalize the energy of the nine branches. The availability of this consideration is equivalent to the solvability of the linear equation in (29).

Assume modulation rate m as,

$$m=\hat{v}_{m2}/\hat{v}_{m1}\geq 0 \quad (32)$$

It is proved that the mentioned consideration is possible under following conditions:

✓ $m\neq 1$

In this condition, the matrix **[A]** is invertible. The reallocated circulating currents would be

$$[\mathbf{i_b}]^*=\mathbf{[A]}^{-1}\cdot\mathbf{[B]}\cdot[\mathbf{e_n}] \quad (33)$$

✓ $m=1,\ \sin\varphi=0$

In this condition, (29) develops multiple solutions. The basic current allocation is one of the solution. Take branches 1, 5 and 9 for instance, as shown in Fig. 4, condition (23) holds because branch currents $\vec{i}_{b1}$, $\vec{i}_{b5}$ and $\vec{i}_{b9}$ are in the same or opposite direction with $\vec{e}_{n1}$, $\vec{e}_{n5}$ and $\vec{e}_{n9}$ respectively.

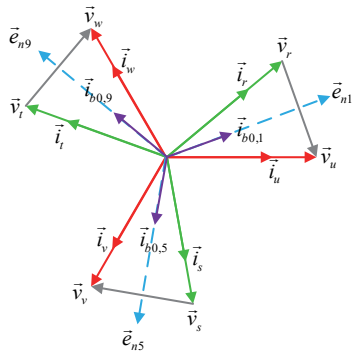

Fig. 4. Phasor Diagram of $m=1,\ \sin\varphi=0$

✓ $m=1,\ \sin\varphi\neq 0,\ \theta=0$ or -120° or 120°

This condition consists of three special cases. Take $\theta=0$ for an instance. In this case, if short branches 1, 5 and 9 and block other branches, there would not be any branch energy fluctuation. For cases of $\theta=-120^\circ$ and $\theta=120^\circ$, the shorted branches should be 2, 6, 7 and 3, 4, 8 respectively.

Impossible condition:

● $m=1,\ \sin\varphi\neq 0,\ \theta\neq 0,-120^\circ,120^\circ$

The mentioned consideration is impossible under this condition. In this case, reactive power or the common-voltage are necessary for the mitigation of the capacitor-voltage fluctuation.

IV. Proposed Control Method

According to PART III.C, if the voltage magnitude of the input side and output side are not identical, the application of branch reallocation in (33) overcomes the capacitor-voltage fluctuation when output frequency gets close to the input frequency.

The theoretical calculation process in the phasor-domain explained in PART III is redesigned into a real-time control method. The control block is shown in Fig. 5. Here an added branch power compensation control is complemented as shown in dashed frame in Fig. 5. The directions of $[\mathbf{e_n}]$ are slightly adjusted to regulate branch energies. Compared to existing control method, the proposed control do not design circulating currents on the basis of basic branch currents. Instead, it firstly moves the M3C close to the branch energy equilibrium point by applying the reallocated branch currents. Then the control method slightly adjusts circulating currents to realize the final branch energy equalization.

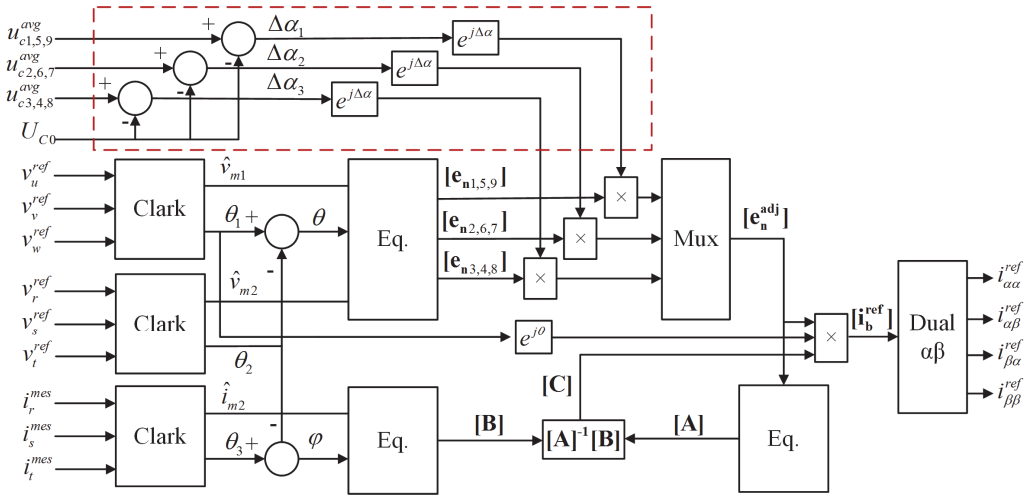

Fig. 5. Proposed Control for the M3C

V. Simulation Results

To verify the theoretical analysis and the proposed control method, simulations studies are conducted in PLECS environment. Simulation parameters are shown in Tab. 1. In Fig. 1, the input side of the M3C is connected to the grid and the output side is connected to a RL-load.

TABLE I. Simulation Parameters

Parameters	Symbols	Value
Switching Frequency	fs	2kHz
Sub-modules per branch	N	1
Module Capacitance	C	1mF
Branch inductance	L_b	5mH
Grid-connected inductance	L_s	5mH
Capacitor Voltage	U_{C0}	500V
Input frequency	f_1	50Hz
Input Voltage Magnitude	$\hat{v}_{m1}$	220V
Output Voltage Magnitude	$\hat{v}_{m2}$	150V
Output Current Magnitude	$\hat{i}_{m2}$	20A

The validity of the proposed control strategy is verified under different operating conditions. Six test operating conditions are set up in Tab .2. The output frequency f_2 is set to be identical or near to the input frequency. Reactive power is applied at the output side.

TABLE II. Test Conditions of the Proposed Control

Test Condition	f_2	$\cos\varphi$
a	50Hz	1
b	50Hz	0.5
c	49Hz	1
d	49Hz	0.5
e	51Hz	1
f	51Hz	0.5

Corresponding simulation results are presented in Fig. 6. In Fig.6 before 0.4 s, the basics current allocation is applied. At 0.4 s, the proposed control strategy is added and the capacitor voltage fluctuation is effectively suppressed in ± 15V in around 0.1s.

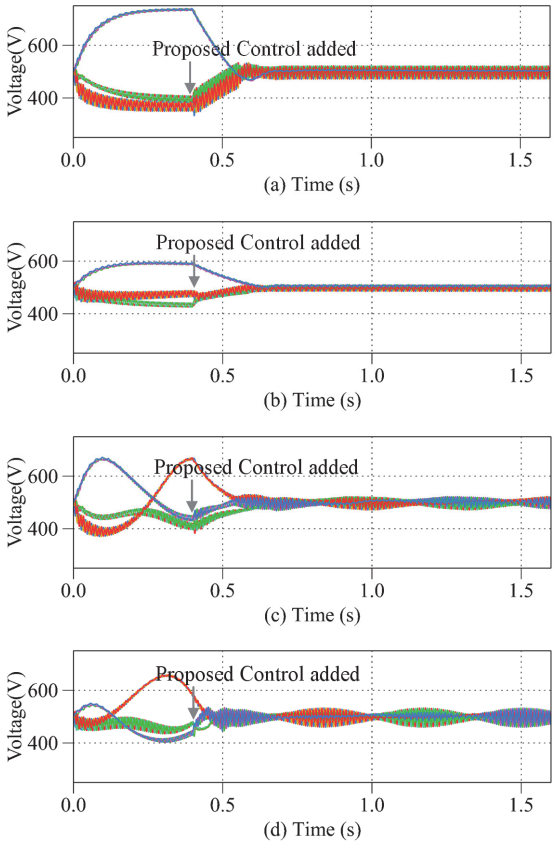

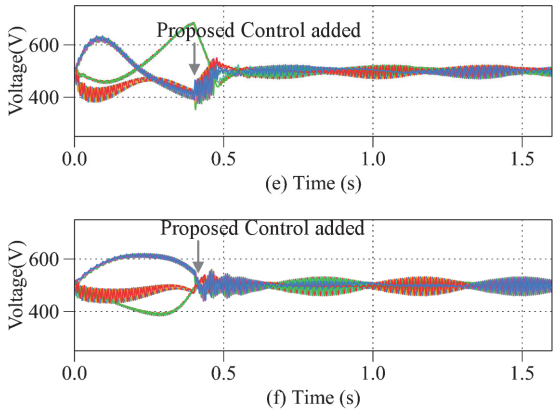

Fig. 6 Nine Branch Capacitor Voltages

(a) $f_2 = 50\text{Hz},\ \cos\varphi = 1$, (b) $f_2 = 50\text{Hz},\ \cos\varphi = 0.5$, (c) $f_2 = 49\text{Hz},\ \cos\varphi = 1$, (d) $f_2 = 49\text{Hz},\ \cos\varphi = 0.5$, (e) $f_2 = 51\text{Hz},\ \cos\varphi = 1$, (f) $f_2 = 51\text{Hz},\ \cos\varphi = 0.5$

The proposed control does not apply reactive power at the input side. For instance, under test condition (b), input voltages (grid voltages), input currents and branch currents are shown in Fig. 7. As the input voltages are in-phase with the output currents, it proves no reactive power at the input side.

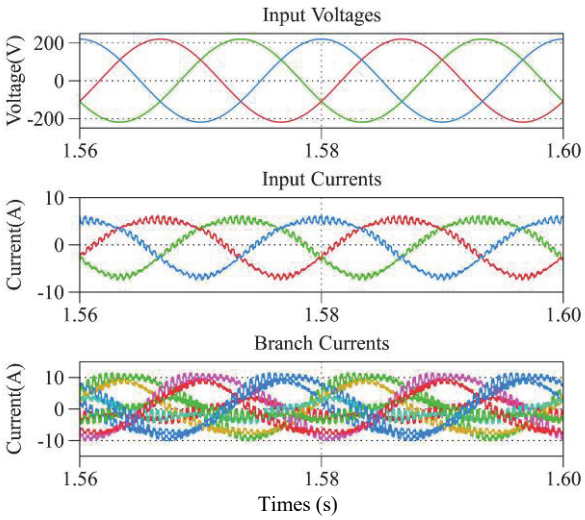

Fig. 7. Simulation results under test condition (b)

VI. Conclusion

This paper has presented a theoretical analysis in the phasor-domain to find the branch energy equilibrium point for the M3C when operating with close input and output frequencies. On the basis of this equilibrium point, a branch current reallocation based energy balancing control strategy has been proposed. The availability of the control strategy is verified. Using this control strategy, the M3C can effectively overcome the capacitor voltage fluctuation without using common mode voltage or applying reactive power at the input side.

References

[1] F. Kammerer, J. Kolb, and M. Braun, "Fully decoupled current control and energy balancing of the modular multilevel matrix converter," in Conf. Rec. IEEE-EPE-PEMC 2012, LS2a.3.

[2] W. Kawamura, M. Hagiwara, and H. Akagi, "A broad range of frequency control for the modular multilevel cascade converter based on triple-star bridge-cells (MMCC-TSBC)," in Conf. Rec. IEEE-ECCE 2013, pp. 4014–4021.

[3] W. Kawamura, M. Hagiwara, and H. Akagi, "Control and experiment of a 380-V, 15-kW motor drive using modular multilevel cascade converter based on triple-star bridge cells (MMCC-TSBC)," in Proc. IPEC 2014, pp. 3742–3749

[4] F. Kammerer, M. Gommeringer, J. Kolb, and M. Braun, "Energy balancing of the modular multilevel matrix converter based on a new transformed arm power analysis," in Conf. Rec. EPE 2014, pp. 1–10.

[5] K. Ilves, L. Bessegato, and S. Norrga, "Comparison of cascaded multilevel converter topologies for ac/ac conversion," in Conf. Rec. IPEC 2014, pp. 1087–1094.

[6] Y. Okazaki, W. Kawamura, M. Hagiwara, H. Akagi, T. Ishida, M. Tsukakoshi, and R. Nakamura, "Which is more suitable for MMCC-based medium-voltage motor drives, a DSCC inverter or a TSBC converter?," in Conf. Rec. ICPE 2015, WeA2-1.

[7] K. Wang, Y. Li, Z. Zheng, and L. Xu, "Voltage Balancing and Fluctuation-Suppression Methods of Floating Capacitors in a New Modular Multilevel Converter," IEEE Transactions on Industrial Electronics, vol. 60, no. 5. pp. 1943–1954, 2013.

[8] W. Kawamura, Y. Chiba, M. Hagiwara, and H. Akagi, "Experimental verification of TSBC-based electrical drives when the motor frequency is passing through, or equal to, the supply frequency," 2015 IEEE Energy Conversion Congress and Exposition (ECCE). pp. 5490–5497, 2015.

[9] M. Diaz, S. Jose, C. Rica, A. Mora, and F. Rojas, "A novel LVRT control strategy for Modular Multilevel Matrix Converter based high-power Wind Energy Conversion Systems," Ecological Vehicles and Renewable Energies (EVER), 2015 Tenth International Conference on. pp. 1–11, 2015.